



## Article

# Preparation and Antimicrobial Properties of Alginate and Serum Albumin/Glutaraldehyde Hydrogels Impregnated with Silver(I) Ions

Louise Gallagher<sup>1</sup>, Alanna Smith<sup>2</sup>, Kevin Kavanagh<sup>2,3</sup>, Michael Devereux<sup>4</sup>, John Colleran<sup>5,6</sup>, Carmel Breslin<sup>1,3</sup> , Karl G. Richards<sup>7</sup> , Malachy McCann<sup>1</sup> and A. Denise Rooney<sup>1,3,\*</sup>

- <sup>1</sup> Department of Chemistry, Maynooth University, Maynooth, W23 F2K8 Co. Kildare, Ireland; louiseannegallagher@gmail.com (L.G.); carmel.breslin@mu.ie (C.B.); malachy.mccann@mu.ie (M.M.)
- <sup>2</sup> Department of Biology, Maynooth University, Maynooth, W23 F2K8 Co. Kildare, Ireland; chemistry.department@mu.ie (A.S.); kevin.kavanagh@mu.ie (K.K.)
- <sup>3</sup> Kathleen Lonsdale Institute for Human Health Research, Maynooth University, Maynooth, W23 F2K8 Co. Kildare, Ireland
- <sup>4</sup> The Centre for Biomimetic & Therapeutic Research, Focas Research Institute, Technological University Dublin-City Campus, D09 V209 Dublin, Ireland; michael.devereux@TUDublin.ie
- <sup>5</sup> School of Chemical & Pharmaceutical Sciences, Technological University Dublin-City Campus, D09 V209 Dublin, Ireland; john.colleran@TUDublin.ie
- <sup>6</sup> Applied Electrochemistry Group, Focas Research Institute, Technological University Dublin, D24 FKT9 Dublin, Ireland
- <sup>7</sup> Environment, Soils and Land-Use Department, Environment Research Centre, Teagasc, Johnstown Castle, Y35 TC97 Wexford, Ireland; Karl.Richards@teagasc.ie
- \* Correspondence: denise.rooney@mu.ie



**Citation:** Gallagher, L.; Smith, A.; Kavanagh, K.; Devereux, M.; Colleran, J.; Breslin, C.; Richards, K.G.; McCann, M.; Rooney, A.D. Preparation and Antimicrobial Properties of Alginate and Serum Albumin/Glutaraldehyde Hydrogels Impregnated with Silver(I) Ions. *Chemistry* **2021**, *3*, 672–686. <https://doi.org/10.3390/chemistry3020047>

Academic Editors: Simona Concilio and Jennifer R. Hiscock

Received: 3 April 2021  
Accepted: 1 June 2021  
Published: 14 June 2021

**Publisher's Note:** MDPI stays neutral with regard to jurisdictional claims in published maps and institutional affiliations.



**Copyright:** © 2021 by the authors. Licensee MDPI, Basel, Switzerland. This article is an open access article distributed under the terms and conditions of the Creative Commons Attribution (CC BY) license (<https://creativecommons.org/licenses/by/4.0/>).

**Abstract:** Calcium alginate (CaALG) hydrogel beads and two sets of composite beads, formed from a combination of calcium alginate/propylene glycol alginate/human serum albumin (CaALG/PGA/HSA) and from calcium alginate with the quaternary ammonium salt, (3-(trimethoxysilyl)propyl)-octadecyldimethylammonium chloride (QA), (CaALG/QA), were prepared. Bovine serum albumin (BSA) was condensed with glutaraldehyde (GLA) to form a BSA/GLA hydrogel. The corresponding Ag<sup>+</sup>-containing gels of all of the above hydrogels were also formed, and slow leaching of the biocidal transition metal ion from the gels bestowed broad spectrum antimicrobial activity. In the absence of added Ag<sup>+</sup>, CaALG/QA was the only material to deliver marginal to moderate antibacterial and antifungal effects. The Ag<sup>+</sup> impregnated hydrogel systems have the potential to maintain the antimicrobial properties of silver, minimising the risk of toxicity, and act as reservoirs to afford ongoing sterility.

**Keywords:** hydrogel; alginate; BSA; glutaraldehyde; silver; antimicrobial

## 1. Introduction

In a medicinal context, there is currently much interest in naturally occurring hydrogels of carbohydrate (e.g., alginate, chitosan) and protein (e.g., serum albumin) origin, as they tend to be non-toxic, biocompatible and biodegradable [1–3]. Moreover, there is extensive current interest in enhancing the properties of these biopolymers by incorporating antimicrobial agents into the polymer matrix for applications in food packaging, wound dressings, and drug delivery [4–6]. With increasing antimicrobial resistance to conventional antibiotics becoming a global healthcare problem, there has been a resurgence in the study of metal based complexes as antimicrobial agents [7]. Having biocidal Ag<sup>+</sup> ions/Ag nanoparticles reside in the hydrogel can offer a dual functionality: they are able to maintain sterility of the material itself, as well as being a reservoir for the slow, sustained delivery of the therapeutic metal cation to targeted microbial pathogens [8–10]. The strong binding affinity of the Ag<sup>+</sup> ion for protein thiol functionalities is known to be central to its

non-specific, multimodal antimicrobial action and to the ultimate demise of the microorganism [11–16]. This disinfectant property, coupled with a relatively high toxicity threshold for mammalian cells (murine model LD<sub>50</sub> values for AgCN, AgNO<sub>3</sub>, and Ag<sub>2</sub>O are 123, 129, and 2820 mg kg<sup>-1</sup>, respectively), makes Ag<sup>+</sup> a good candidate for incorporation into antimicrobial hydrogels [17,18].

Bovine serum albumin (BSA) crosslinked with glutaraldehyde (GLA) [19,20] is a well-known wound adhesive hydrogel (abbreviated here as BSA/GLA) and is marketed by CryoLife Inc. under the name BioGlue [21]. The product gained approval from the US Food and Drug Administration (FDA) in 2001 and is widely used as an adhesive in surgeries such as those that involve the repair of the aorta, femoral, and carotid arteries [22,23]. However, it has been reported that an increase (5.4%) in surgical site infections occurred when BioGlue was used on patients undergoing craniotomy, and that this returned to the normal rate of 1% when its use was discontinued [24]. A wide variety of microorganisms were found to be responsible for infection, and it was concluded that the BSA/GLA hydrogel adhesive promotes an inflammatory response, causing subsequent wound breaches and permitting microbes to spread down into the wound. When we prepared a sample of this BSA/GLA hydrogel in our laboratory it was seen that, upon standing in the atmosphere at ambient temperature for a few days, a substantial surface coverage of microbial growth developed (Figure 1), indicating that the glue formulation was a good growth medium for microorganisms. This observation prompted us to explore the possibility of incorporating antimicrobially-active Ag<sup>+</sup> ions into the BSA/GLA hydrogel formulation in order to retain both product and wound site sterility during surgical use.

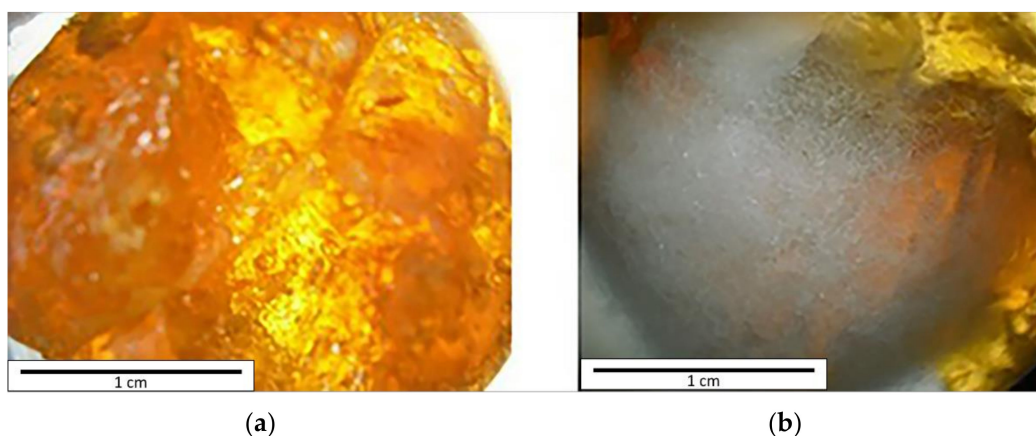


**Figure 1.** Photographs of the surfaces of BSA/GLA hydrogels prepared in accordance with the formulation specified for commercial BioGlue: (a) freshly prepared BSA/GLA hydrogel and (b) surface fungal contamination (grey) of a BSA/GLA sample left standing in the atmosphere for 4 days.

Described herein is the synthesis and antimicrobial screening of some alginate (ALG) and BSA/GLA hydrogels which have been infused with Ag<sup>+</sup> cations. We report a novel silver impregnated antimicrobial adaptation of the commercially available bio-adhesive (albumin-glutaraldehyde) BioGlue. In addition, there is intensive research interest in developing and using alginate-based hydrogel materials containing silver, and a huge number of studies have investigated the antimicrobial properties of alginates [25]. However, to the best of our knowledge, the current study is the first report of an investigation into the broad-spectrum antimicrobial properties of silver impregnated hydrogels formed containing chemically modified alginate hydrogels, serum-albumin-propylene glycol alginate, and the alginate-quaternary ammonium complex (Figure 2).

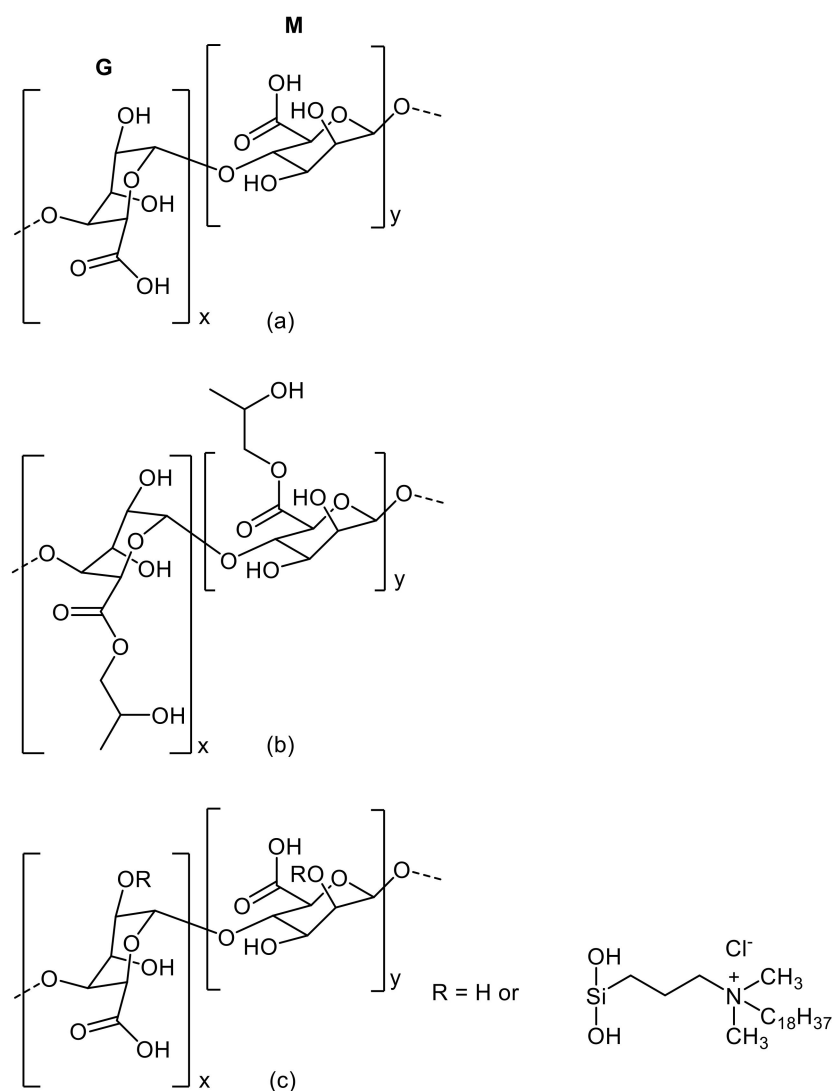


**Figure 2.** (a) Alginate block co-polymer containing monomers of  $\beta$ -D-mannuronic acid (M) and  $\alpha$ -L-guluronic acid (G) joined by a 1,4-glycosidic linkage. (b) Alginate esterified with propylene glycol to give propylene glycol alginate (PGA) (esterification (70%) occurs at both the M and G residues). (c) Alginate reacted with (3-(trimethoxysilyl)propyl)-octadecyldimethylammonium chloride (TSA) to give the corresponding quaternary ammonium salt (ALG/QA). (Note c shows the TSA anchored at one OH group on the alginate but it could potentially react with more than one alginate OH group).

## 2. Materials and Methods

Unless otherwise stated, chemicals and solvents were purchased from commercial sources and used without further purification. Calibration grade  $\text{AgNO}_3$  (99.9999%) was used for atomic absorption spectroscopy. Sodium alginate, with a viscosity of 20–40 cps and a concentration of 1% *w/v* in  $\text{H}_2\text{O}$ , was used. Propylene glycol alginate with 70% esterification was obtained from Wako. Millipore deionised water was used for hydrogel and solution preparations. All  $\text{Ag}^+$ -containing hydrogels were prepared in the absence of light and samples were stored in the dark. Surface characterisation of the alginate hydrogel beads was carried out using scanning electron microscopy (SEM) and energy-dispersive X-ray (EDX) analysis, and the instrument used was a Hitachi S-3200-N (UK) containing a tungsten filament electron source, giving a maximum magnification of 300,000 and a resolution of 3.5 nm. This microscope was equipped with an Oxford Instrument INCAx-act EDX system with a silicon drift detector. The size limits of the dried alginate beads (samples of 100 beads) were determined using a Gilsonic auto sieve. Dry alginate hydrogel

beads were also examined optically with a LeicaDMEP DFC-280 (Wetzlar, Germany) and an Olympus BX51M system (UK) using Leica application suite (Wetzlar, Germany) and Olympus DP Version 3.2 software (UK). The diameters of 20 beads were measured using an Olympus BX51M Microscope, and a similar diameter range was found to that obtained with the Gilsonic auto sieve. Infrared spectra were recorded, as either KBr discs or as liquid films between NaCl plates, using a Perkin Elmer system 2000 FT-IR spectrometer (Waltham, MA, USA). CHN elemental analysis was performed using a Flash EA 1112 Series Elemental Analyser (Waltham, MA, USA) aligned with Eager 300 Operating Software (Waltham, MA, USA).

Quantitative  $\text{Ag}^+$  ion content was measured using either atomic absorption (AA) spectroscopy (Perkin Elmer AAnalyst 200 atomic absorption spectrometer) or electrochemically by anodic stripping voltammetry (CH Instruments Electrochemical Workstation and a CHI760c data analysis program). For AA measurements, dry, pre-weighed alginate/ $\text{Ag}^+$  and BSA/GLA/ $\text{Ag}^+$  samples were ashed in a ceramic crucible over a Bunsen burner and the residue dissolved in aqueous nitric acid (20 mL, 50% *v/v*). After cooling, the acid solutions were gravity filtered into a 250 cm<sup>3</sup> volumetric flask and made up to the mark using deionised water. From this stock solution, a 1 in 25 dilution was carried out and the silver content measured against a standard curve produced using known concentrations of  $\text{AgNO}_3$ .

For  $\text{Ag}^+$  ion determination using anodic stripping voltammetry (BSA/GLA/ $\text{Ag}^+$  samples only), a method similar to that described by Holt and Bard was followed [26]. All experiments were performed in a Faraday Cage and the cell was covered in aluminium foil to ensure experimental data were obtained in the absence of light. Optimisation of the electrochemical parameters,  $\text{Ag}^+$  deposition times and potential, and the anodic stripping potential windows, was achieved using cyclic voltammetry, constant potential voltammetry, and linear sweep voltammetry (supplementary information, Figures S1 and S2). Stripping peak currents (for generation of calibration curves and leaching experiments) were normalised with respect to the experimental deposition times, and linear calibration curves were generated from standard  $\text{AgNO}_3$  solutions (Figure S3). An in situ electrochemical electrode cleaning step was performed between each data point acquisition.

Silver ion leaching from the hydrogel disks was monitored electrochemically over 55-h periods (Figure S4). All disks were of equal mass (0.1 g) and were encased beneath a platinum mesh (inert), which was immobilized at the base of the electrochemical cell. The mesh cage ensured that the hydrogels remained separated from the electrodes and limited enforced leaching due to convection currents that may have arisen through manipulation of the working electrode throughout the duration of the experiments. The total solution volume in the cell was 60 cm<sup>3</sup> and after each stripping protocol the electrodes were removed from the solution, polished, and dried prior to subsequent measurements. Application of the aforementioned electrochemical cleaning step potential ( $E_{\text{app}} = 0.9 \text{ V}$  for 1 min) ensured no silver remained on the electrode surface prior to polishing between measurements. The equation of the line,  $I_p/t = 1.42 \pm 0.04 \times 10^{-3} \text{ M}^{-1} [\text{Ag}] + 5.54 \pm 0.10 \times 10^{-10} \text{ A/s}$ , was then used to quantify concentrations of  $\text{Ag}^+$  leaching from the BSA/GLA/ $\text{Ag}^+$  samples over time.

## 2.1. Hydrogel Synthesis

### 2.1.1. Calcium Alginate (CaALG) Hydrogel Beads

CaALG hydrogel beads were prepared using adaptations of literature procedures [27–29]. An aqueous solution of sodium alginate (30 mL, 2% *w/v*) was added dropwise from a syringe (no needle attached) into a  $\text{CaCl}_2$  solution (0.25 M, 100 mL). The distance between the surface of the  $\text{CaCl}_2$  solution and the bottom of the syringe was fixed at 60 mm and the drop rate was maintained at 0.2 mL/min. The spherical beads were formed under magnetic stirring for 0.5 h. Freshly formed beads ( $n = 500$ ) were kept immersed in  $\text{CaCl}_2$  solution (5% *w/v*) for 24 h. The beads were then removed by filtration and repeatedly

washed with deionised water to remove any excess  $\text{CaCl}_2$  solution. These beads were stored in the presence of residual deionised water for further use.

#### 2.1.2. Calcium Alginate/Propylene Glycol Alginate/Human Serum Albumin Composite Beads (CaALG/PGA/HSA)

Propylene glycol alginate (PGA) is a partially esterified derivative formed from the reaction between propylene oxide and alginic acid in which ca. 70% of the carboxylic groups are esterified with propylene glycol [30]. The beads were formed by an adaptation of the method developed by Edwards-Levy et al. [31]. Sodium alginate (1.0 g) was dissolved in deionised water (100 mL). Aqueous PGA solution (100 mL, 2% *w/v*) was added, followed by a solution of human serum albumin (HSA) (5 mL, 5% *v/v*). The mixture was stirred at room temperature for 24 h. The resulting viscous solution (30 mL) was placed in a syringe and added dropwise into a  $\text{CaCl}_2$  solution (100 mL, 10% *w/v*). For optimum bead formation, the distance between the  $\text{CaCl}_2$  solution and the bottom of the syringe was fixed at 60 mm and the drop rate was 0.2 mL/min. The beads ( $n = 350$ ) were formed under magnetic stirring for 0.5 h, filtered off, and then washed repeatedly with deionised water. The resulting opaque beads were added to a freshly prepared sodium hydroxide solution (100 mL, 0.025 M) and stirred for 0.25 h. The beads changed to a white colour instantaneously upon contact with the sodium hydroxide solution, due to the reaction of the HSA with the PGA in the basic medium. The beads were filtered off and placed in a buffer solution (pH 7) for 0.25 h. After filtration, they were washed repeatedly with deionised water to remove any excess solution from the surface. The beads were kept in their hydrogel state by being stored in the presence of residual deionised water.

#### 2.1.3. Calcium Alginate/Quaternary Ammonium Alginate Composite Hydrogel Beads (CaALG/QA)

Alginate containing quaternary ammonium groups was prepared by the reaction of sodium alginate with (3-(trimethoxysilyl)propyl)-octadecyldimethylammonium chloride in acid solution. This reaction anchors the quaternary ammonium group to the polymer backbone by a covalent, non-hydrolysable bond. CaALG/QA beads were prepared according to the method developed by Kim et al. [32]. Sodium alginate (4.0 g) was slowly added to stirred deionised water (100 mL), and to this was added an aqueous solution of (3-(trimethoxysilyl)propyl)-octadecyldimethylammonium chloride (41 mL, 0.02 M). An aqueous solution of acetic acid (0.8 M) was then added at room temperature to reduce the pH to 4. The mixture changed from pale yellow to a milky white colour and was left stirring for 24 h. The resulting viscous solution (30 mL) was placed into a syringe (no needle attached) and dispensed dropwise into a solution of  $\text{CaCl}_2$  (100 mL, ca. 5% *w/v*). The distance between the  $\text{CaCl}_2$  solution surface and the bottom of the syringe was 60 mm, and the drop rate was 0.2 mL/min. Smooth, spherical beads formed under magnetic stirring for 0.5 h. Freshly formed beads ( $n = 350$ ) were kept immersed in  $\text{CaCl}_2$  solution (ca. 5% *w/v*) for 24 h. The beads were then removed by filtration and repeatedly washed with deionised water to remove any excess  $\text{CaCl}_2$  solution.

Before  $\text{Ag}^+$  ions could be incorporated into the CaALG/QA composite beads, the chloride counterions associated with the quaternary ammonium groups were exchanged for nitrate ions to avoid  $\text{AgCl}$  precipitation. The composite beads were placed into an ion exchange tube and washed continuously with nitric acid (0.05 M) until chloride ions were reduced (as determined by EDX analysis). These beads were stored in the presence of residual deionised water.

#### 2.1.4. Determination of the Swelling Ratio (%) of Alginate Xerogel Beads

The swelling ratio of the beads was studied by the measurement of the equilibrium swelling degree (ESD%) which was calculated according to Equation (1) [33,34]:

$$\text{ESD}\% = (W_s - W_d)/W_d \times 100 \quad (1)$$

where  $W_s$  is the weight of swollen beads after reaching equilibrium swelling degree and  $W_d$  is the dry weight of the hydrogel beads. ESD values for individual formulations of the beads were determined by measuring the extent of swelling of the beads in the different swelling media at  $20 \pm 1$  °C. The different swelling media used were deionised water, and sodium chloride (1% *w/v*) solution. Fully dried xerogels ( $n = 20$ ) were weighed using a balance with 0.1 mg accuracy. The water in the water bath was allowed to equilibrate to  $20 \pm 1$  °C before the swelling study was conducted. Swelling studies were conducted by placing the beads in 20 mL of the swelling media at a temperature of  $20 \pm 1$  °C unless otherwise stated. To calculate their weight at a given time, the beads were filtered using gravity filtration, and extraneous water was removed using filter paper. The beads were then weighed using a balance with 0.1 mg accuracy. The studies were carried out in triplicate.

### 2.2. Preparation of $Ag^+$ -Containing Alginate Beads

All of the  $Ag^+$ -containing alginate hydrogel beads were prepared in accordance with the method outlined below for the synthesis of CaALG/ $Ag^+$  (0.01) and CaALG/ $Ag^+$ (0.1). CaALG beads ( $n = 100$ ) were immersed in a stirred solution of  $AgNO_3$  (0.1 M or 0.01 M) for 3 h (24 h in the case of CaALG/QA/ $Ag^+$ ). The beads were then washed with deionised water to remove any residual surface  $Ag^+$  solution. The presence of  $Ag^+$  within the beads was confirmed by EDX spectroscopy, and the mass of  $Ag^+$  encapsulated in the beads was determined using AA spectroscopy. A quantity of hydrogel beads were removed from storage, placed in an oven, and weighed periodically until there was no further reduction in weight.

### 2.3. $Ag^+$ Leaching from Alginate Hydrogels

AA spectroscopy was used to quantify the amount of  $Ag^+$  ion released from the  $Ag^+$ -containing alginate beads. Beads ( $n = 30$ ) were suspended in deionised water (10 mL) at 30 °C for 24 h and without stirring. The beads were filtered off and the filtrate was made up to 100 mL. Absorbance readings were taken and, using a calibration curve determined using known concentrations of  $AgNO_3$ , the mass of  $Ag^+$  leached from the beads was calculated. The experiments were repeated in triplicate and the average of the three readings was recorded.

### 2.4. Preparation of BSA/GLA Hydrogel

BSA (0.50 g,  $7.46 \times 10^{-3}$  mmoles) was added to distilled water (2.0 mL) and the mixture vortexed until the solid had completely dissolved. A solution of glutaraldehyde (GLA) (0.11 g, 1.09 mmole) was prepared in distilled water (1 mL). The GLA solution (0.25 mL) was slowly pipetted into the BSA solution. The mixture was vortexed briefly and after ca. 2 min the golden-coloured hydrogel formed. The sample was dried under high vacuum to a constant weight (0.49 g) to form the respective xerogel.

### 2.5. Preparation of $Ag^+$ -Containing BSA/GLA/ $Ag^+$ Hydrogels

The separate BSA and GLA solutions were prepared as described above. A solution of  $AgNO_3$  (1.0 mL, containing 0.01 g  $AgNO_3$ ) was added to the GLA solution (0.25 mL). This GLA/ $AgNO_3$  solution was then slowly added to the BSA solution and the resulting BSA/GLA/ $Ag^+$ (0.01) hydrogel vortexed briefly. The sample was dried under high vacuum to a constant dry weight (0.57 g) and stored in the dark. This procedure was repeated using 0.001 g  $AgNO_3$  to give the BSA/GLA/ $Ag^+$ (0.001) hydrogel, and again was dried to a dry weight of 0.57 g. The final  $Ag^+$  content in the 0.57 g dry samples of BSA/GLA/ $Ag^+$ (0.01) and BSA/GLA/ $Ag^+$ (0.001) was  $5.88 \times 10^{-5}$  moles  $Ag^+$  and  $5.88 \times 10^{-6}$  moles  $Ag^+$ , respectively. The amount of  $Ag^+$  ion in the formulations of BSA/GLA/ $Ag^+$ (0.01) and BSA/GLA/ $Ag^+$ (0.001) hydrogels did not appear to compromise their adhesive properties when compared to the BSA/GLA gel formulated without added  $Ag^+$  ions. In contrast, a BSA/GLA/ $Ag^+$ (0.1) mixture, prepared using 0.1 g  $AgNO_3$ , formed a non-swelling,

non-adhesive paste rather than a proper hydrogel glue. This is most likely a result of additional, constricting, metal ion-bridged crosslinking within the polymer network [35]. BSA/GLA/Ag<sup>+</sup>(0.1) was not investigated further.

All BSA/GLA and BSA/GLA/Ag<sup>+</sup> hydrogels were freshly prepared prior to the biological screening studies.

#### 2.6. Ag<sup>+</sup> Leaching from BSA/GLA/Ag<sup>+</sup> Hydrogels

To prevent the possibility of Ag<sup>+</sup> photoreduction, the complete electrochemical cell assembly was covered in aluminium foil throughout the duration of each experiment, including during electrode polishing. Anodic stripping voltammetry was carried out to quantify the amount of Ag<sup>+</sup> ions leached from BSA/GLA/Ag<sup>+</sup> samples over time. For example, BSA/GLA/Ag<sup>+</sup>(0.01) (dry mass 0.10 g and containing  $1.03 \times 10^{-5}$  moles Ag<sup>+</sup> ions) was placed in the electrochemical cell and a supporting electrolyte (60 mL) was added (if all of the Ag<sup>+</sup> ions were leached from the material,  $1.03 \times 10^{-5}$  moles of Ag<sup>+</sup> ions would be released). A mass of 0.10 g of the dry BSA/GLA/Ag<sup>+</sup>(0.001) sample could possibly release a maximum of  $1.03 \times 10^{-6}$  moles of Ag<sup>+</sup> ions into the supporting electrolyte. The quantity of Ag<sup>+</sup> ions leached into the electrolyte was determined at time intervals of up to 55 h and the experiments were conducted in duplicate.

#### 2.7. Biological Studies

The following yeast and bacterial strains were used: *Candida albicans* 10231, American Type Culture Collection (ATCC), Marassas, VA, USA; gram-positive Methicillin-resistant *Staphylococcus aureus* (MRSA) (ATCC); gram-positive *Staphylococcus aureus* (clinical isolate, urinary tract infection, St. James's Hospital, Dublin, Ireland); gram-negative *Escherichia coli* (clinical isolate, gastro-intestinal tract infection, St. James's Hospital, Dublin, Ireland); gram-negative *Pseudomonas aeruginosa* 10145 and 27853 (ATCC). The disc diffusion antimicrobial testing protocol was used to screen the test materials against these microorganisms.

Sterilisation of microbiological equipment and media was carried out in a Dixons ST2228 autoclave at 121 °C and 124 kPa for 20 min. All worktops and benches were sterilised by washing with ethanol/water (70% v/v) prior to use. Fungal cell density was measured using a Neubauer hemocytometer under a light microscope at a magnification of  $\times 400$ . Bacterial cell density was recorded at an optical density of 600 nm (OD<sub>600</sub>) using an Eppendorf Biophotometer.

#### 2.8. Anti-Candida Testing

Deionised water was used to make up all media. *C. albicans* was grown on yeast extract peptone dextrose (YEPD) agar plates at 37 °C and maintained at 4 °C for short term storage. Cultures were routinely sub-cultured every 4–6 weeks. Cultures were grown to the stationary phase at 37 °C, and the fungal cells were added to the YEPD plates at a concentration of  $1 \times 10^6$  cells/mL. The plates were incubated for 1 h at 37 °C and the test sample was then placed on the plate. In the case of the alginate samples, freshly made swollen beads were used (if dried beads are used, the zone of inhibition is very small, suggesting that Ag<sup>+</sup> ions are unable to efficiently leach out of dried beads, whereas pores are open in swollen beads, enabling Ag<sup>+</sup> ions to leach out to a greater extent). The plates were then incubated for 24 h at 37 °C, and the zones of inhibition were determined by measuring the area of the sample and the area of the sample plus the zone of inhibition. The area of the sample was then subtracted from the area of the sample plus the zone of inhibition to give the area of the zone of inhibition (mm<sup>2</sup>). This procedure was carried out using three separate samples of each test material and the mean of the readings was tabulated.

#### 2.9. Antibacterial Testing

All bacterial strains were grown on nutrient broth agar plates at 37 °C and maintained at 4 °C for short term storage. Cultures were routinely sub-cultured every 4–6 weeks. Bacteria were grown overnight to the stationary phase in nutrient broth at 37 °C, with

shaking at 200 rpm. The cells were diluted to give an  $OD_{600}$  value of 0.1 and these were then added to the agar plates. The plates were incubated for 1 h at 37 °C, the solid test sample was placed on the plate and incubated for 24 h at 37 °C, and the zones of inhibition were measured. This procedure was repeated on three separate occasions and the mean of the readings was tabulated.

### 3. Results and Discussion

The three sets of alginate hydrogel beads used  $Ca^{2+}$  ions as the major crosslinker, and in the case of CaALG/PGA/HSA, the HSA provided additional crosslinking, which gave the beads greater structural integrity and also offered additional sites for subsequent  $Ag^+$  binding. The FTIR spectrum of the CaALG/QA composite beads showed bands at 908 and 1100  $cm^{-1}$ , consistent with reported values, and which were assigned to Si-O-C and Si-O stretches, respectively. The loss of the O-CH<sub>3</sub> stretching band at 1193  $cm^{-1}$  present in the quaternary ammonium starting material indicates that the SiOCH<sub>3</sub> groups had hydrolysed and the methoxy group was lost (Figure S5) [32]. C-H stretching bands at 2920 and 2851  $cm^{-1}$  for the alkyl groups had increased substantially in intensity compared to those in the spectrum of the sodium alginate (Figure S5). The EDX spectrum of the beads (Figure S6) showed a line at 1.74 keV which is assigned as the  $K_{\alpha 1}$  line of silicon. These findings are consistent with the attachment of the (3-(trimethoxysilyl)propyl)-octadecyldimethylammonium chloride to the alginate chain. In addition, elemental analysis data confirmed the presence of nitrogen and also an increase in the carbon content of CaALG/QA (%C 41.69; %H 7.65; %N 1.62) compared to CaALG (%C 21.91; %H 4.29), which is consistent with the attachment of the long alkyl chains to the alginate. The exchange of the chloride for the nitrate ion for the CaALG/QA beads was followed by the reduction of the chloride signal in the EDX spectrum of the dried bead. The substitution of some of the  $Ca^{2+}$  ions in the various beads with  $Ag^+$  was accomplished by immersing the preformed  $Ca^{2+}$ -containing beads in a solution of  $AgNO_3$  (0.1 or 0.01 M) for a period of 3 h for CaALG and CaALG/PGA/HSA, and 24 h for CaALG/QA. Encapsulation of  $Ag^+$  ions into the alginate hydrogels was confirmed by EDX analysis (Figure S6).

Preparation of the BSA/GLA/ $Ag^+$  hydrogels involved the addition of GLA/ $AgNO_3$  solution to an aqueous solution of BSA (i.e., the  $Ag^+$  ions were incorporated during hydrogel formation as opposed to post treatment of the gel with  $AgNO_3$ , as was the case with the alginate hydrogel beads). It should be noted that if too much  $Ag^+$  ion is used in the synthesis of BSA/GLA/ $Ag^+$  (e.g., using 0.1 M  $AgNO_3$ ), a non-adhesive paste rather than a hydrogel is formed. Adding too little  $Ag^+$  ions during BSA/GLA/ $Ag^+$  hydrogel formation produces a gel that lacks effective antimicrobial protection.

The surface morphologies of the biopolymer materials were recorded when they were in the xerogel form. For the various types of calcium alginate beads, the morphologies of the beads containing added  $Ag^+$  ions were quite similar to the precursor beads without  $Ag^+$ . No significant change in the size of the alginate beads was observed upon impregnation with  $Ag^+$  ions; for example, CaALG and CaALG/ $Ag^+$  beads both had median diameters in the range 600–710  $\mu m$  (determined using sieving experiments). Illustrated in Figure 3 are the SEM micrographs of the three types of  $Ag^+$ -containing alginate beads in their xerogel form, prepared by immersion in 0.1 M  $AgNO_3$  solution. CaALG/ $Ag^+$ (0.1) beads were almost spherical and had a very smooth morphology (Figure 3a,b). In contrast, CaALG/PGA/HSA/ $Ag^+$ (0.1) composite beads (Figure 3c,d) were substantially less symmetrical, possibly due to the increased viscosity of the polymer solution used for the gelling process, and their surface exhibited large folds. CaALG/QA/ $Ag^+$ (0.1) beads, which contain the quaternary ammonium function, had a very granular morphology (Figure 3e,f).



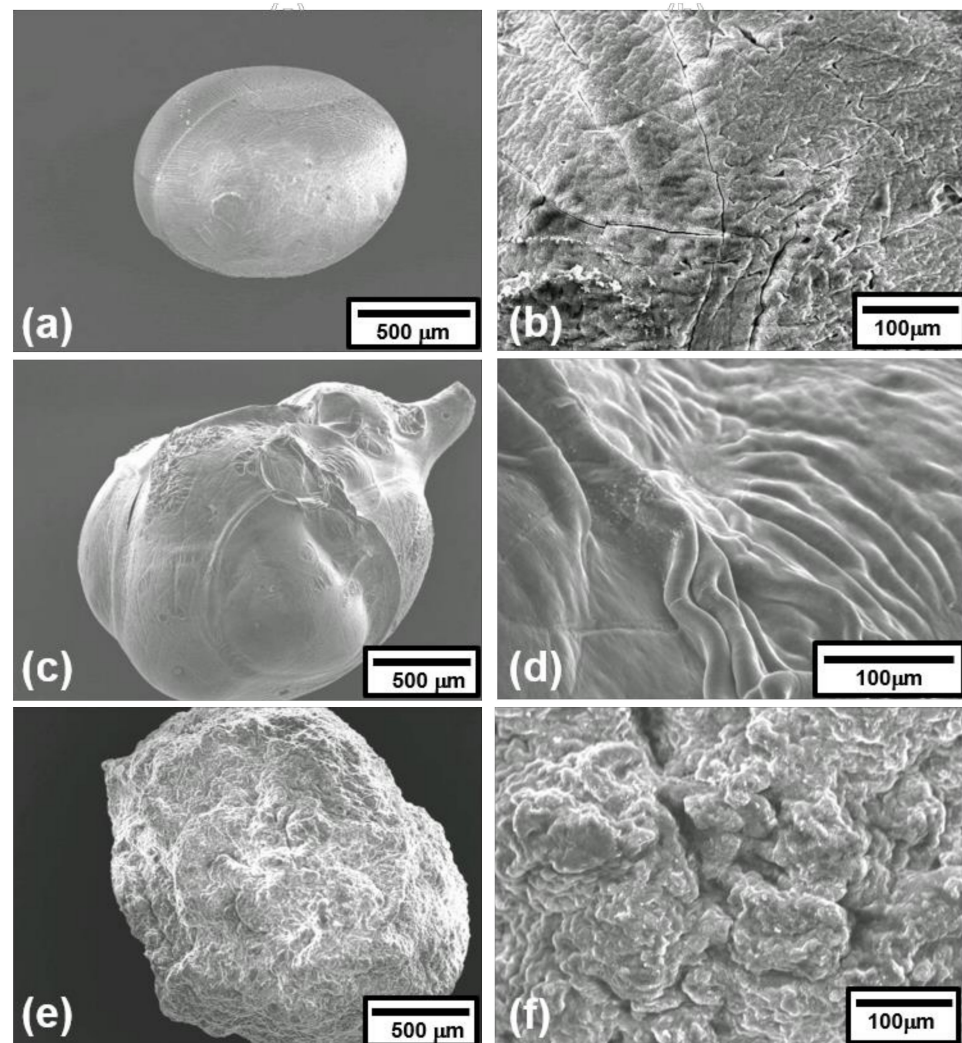


**Figure 3.** SEM images of xerogel alginate beads following incorporation of  $\text{Ag}^+$  ions: (a,b) are CaALG/ $\text{Ag}^+$ (0.1 M); (c,d) are CaALG/PGA/HSA/ $\text{Ag}^+$ (0.1 M); (e,f) are CaALG/QA/ $\text{Ag}^+$ (0.1 M).

SEM images were also obtained for  $\text{Ag}^+$ -free and  $\text{Ag}^+$ -containing BSA/GLA xerogels (Figure 4). The surface of the metal-free BSA/GLA composite (Figure 4a) appeared smooth, although it was quite heterogeneous and contained deep craters of diameter ca. 50  $\mu\text{m}$ . The latter indentations in the desiccated sample were probably the remnants of large water-filled macropores that permeated the former hydrogel [36]. The BSA/GLA/ $\text{Ag}^+$ (0.01) sample (Figure 4b) also had a very smooth surface but lacked crater indentations, possibly reflecting a reduction in porosity and a tighter matrix arising from cross-linking by the resident  $\text{Ag}^+$  ion. In contrast, BSA/GLA/ $\text{Ag}^+$ (0.1), which was prepared using a further 10-fold higher concentration of  $\text{AgNO}_3$ , and which did not form a true hydrogel, had a more rugged appearance, and crystals of  $\text{AgNO}_3$  were clearly recognisable on the surface of the product (image not shown).

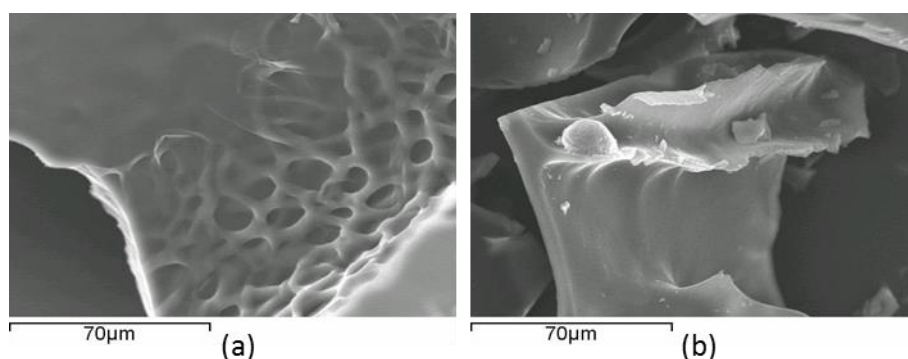


**Figure 4.** SEM images of (a) Ag<sup>+</sup>-free BSA/GLA and (b) BSA/GLA/Ag<sup>+</sup>(0.01).

The equilibrium swelling degree (ESD%) for the three types of alginate beads without silver were recorded after they had been immersed in water or 1% *w/v* NaCl solution at  $20 \pm 1$  °C (Table 1). Over the 8 h study, the three sets of beads increased in mass by a similar amount in the deionised water. In contrast, both the CaALG/PGA/HSA and CaALG/QA swelled to a much smaller extent than the CaALG beads in the 1% *w/v* NaCl solution. Interestingly, the CaALG/QA swelling only marginally increased when going from a solution of deionised water to 1% *w/v* NaCl, indicating that this material is less severely damaged by Na<sup>+</sup> cations. These cations are present in blood at about 0.8% *w/v*.

**Table 1.** ESD% of Alginate-based beads in deionised water and 1% *w/v* NaCl held at  $20 \pm 1$  °C for 8 h.

Medium	CaALG EDS%	CaALG/PGA/HAS EDS%	CaALG/QA EDS%
Deionised Water	59	82	82
1% <i>w/v</i> NaCl	6481	666	120

Data for the uptake and release of Ag<sup>+</sup> ions for the three different classes of Ag<sup>+</sup>-containing alginates are given in Table 2. When comparing the Ag<sup>+</sup> ion uptake of CaALG/Ag<sup>+</sup> and CaALG/PGA/HSA/Ag<sup>+</sup> beads, it appeared that the anticipated decrease in the number of Ag<sup>+</sup>-binding carboxylate moieties in the latter species, as a consequence of esterification (ca. 70%) with the propylene glycol, was balanced by the presence of metal binding domains in the albumin portion of the composite. Following immersion in 0.01 M AgNO<sub>3</sub>, it was found, somewhat unexpectedly, that CaALG/QA/Ag<sup>+</sup>(0.01) retained 3.5 times the amount of Ag<sup>+</sup> ions compared to CaALG/Ag<sup>+</sup>(0.01). However, at the higher concentration of administered AgNO<sub>3</sub> (0.1 M), both materials showed a similar uptake of the metal ion. Although the uptake of Ag<sup>+</sup> from the aqueous AgNO<sub>3</sub> by the three different alginates increased upon raising the initial concentration of the AgNO<sub>3</sub> solution used, this was not a directly proportional relationship. Unexpectedly, for the CaALG/Ag<sup>+</sup>(0.01)-CaALG/Ag<sup>+</sup>(0.1) and CaALG/PGA/HSA/Ag<sup>+</sup>(0.01)-CaALG/PGA/HSA/Ag<sup>+</sup>(0.1) pairings, a 10-fold increase in concentration of added AgNO<sub>3</sub> solution yielded a > 10-fold increase in the uptake of Ag<sup>+</sup> ion (ca. 14- and 23-fold, respectively). In the case of the CaALG/QA/Ag<sup>+</sup>(0.01)-CaALG/QA/Ag<sup>+</sup>(0.1) pair, there was a less dramatic increase in Ag<sup>+</sup> ion uptake (ca. 5-fold).

**Table 2.** Uptake and release of Ag<sup>+</sup> ions for Ag<sup>+</sup>-containing alginates.

Sample	Ag <sup>+</sup> Content in 30 Beads (mg) [Moles]	Ag <sup>+</sup> Leached from 30 Beads (mg) [Moles] {% of Bead Ag <sup>+</sup> Content}
CaALG/Ag <sup>+</sup> (0.01)	8.0 ± 0.5 [7.41 × 10 <sup>-5</sup> ]	0.04 ± 0.01 [3.7 × 10 <sup>-7</sup> ] {0.5}
CaALG/Ag <sup>+</sup> (0.1)	110.0 ± 9.0 [1.02 × 10 <sup>-3</sup> ]	2.24 ± 0.01 [2.1 × 10 <sup>-5</sup> ] {2.0}
CaALG/PGA/HSA/Ag <sup>+</sup> (0.01)	7.3 ± 0.3 [6.8 × 10 <sup>-5</sup> ]	0.03 ± 0.01 [2.8 × 10 <sup>-7</sup> ] {0.4}
CaALG/PGA/HSA/Ag <sup>+</sup> (0.1)	167 ± 22 [1.5 × 10 <sup>-3</sup> ]	3.86 ± 0.02 [3.57 × 10 <sup>-5</sup> ] {2.3}
CaALG/QA/Ag <sup>+</sup> (0.01)	28 ± 5 [2.6 × 10 <sup>-4</sup> ]	1.58 ± 0.01 [1.46 × 10 <sup>-5</sup> ] {5.6}
CaALG/QA/Ag <sup>+</sup> (0.1)	129 ± 7 [1.2 × 10 <sup>-3</sup> ]	2.91 ± 0.01 [2.69 × 10 <sup>-5</sup> ] {2.2}

Quantities of Ag<sup>+</sup> ions leached from the Ag<sup>+</sup>-containing alginate hydrogel beads into deionised water at 30 °C were measured using AA spectroscopy over a period of 24 h and are also summarised in Table 2. Although there was only a 10-fold difference in the concentration of AgNO<sub>3</sub> used in preparing CaALG/Ag<sup>+</sup>(0.01) and CaALG/Ag<sup>+</sup>(0.1) beads, the latter sample liberated 56 times more Ag<sup>+</sup> ions, and the %Ag<sup>+</sup> released were 0.5 and 2.0, respectively. An even more dramatic increase in metal ion release (129 times) was witnessed on progressing from CaALG/PGA/HSA/Ag<sup>+</sup>(0.01) to CaALG/PGA/HSA/Ag<sup>+</sup>(0.1), which equated to 0.4 and 2.4% of the original Ag<sup>+</sup> content, respectively. A more modest increase (ca. 2 times) in the discharge of Ag<sup>+</sup> occurred on going from CaALG/QA/Ag<sup>+</sup>(0.01) to CaALG/QA/Ag<sup>+</sup>(0.1), corresponding to 5.6 and 2.2%, respectively, of the amount of Ag<sup>+</sup> ion originally bound. The %release trend for the CaALG/QA/Ag<sup>+</sup>(0.01)-CaALG/QA/Ag<sup>+</sup>(0.1) pair, in which the sample prepared using the lower initial concentration of AgNO<sub>3</sub> (0.01 M) had the greater %release of Ag<sup>+</sup> ions, was the opposite to that observed for the other two alginate pairings.

The leaching of Ag<sup>+</sup> ions from BSA/GLA/Ag<sup>+</sup>(0.01) and BSA/GLA/Ag<sup>+</sup>(0.001) hydrogels into the aqueous NaNO<sub>3</sub> supporting electrolyte at room temperature were recorded using stripping voltammetry over a number of time points over a 55 h period. For both samples, there was relatively rapid leaching of Ag<sup>+</sup> ions from the materials into the supporting electrolyte over the first hour. Ag<sup>+</sup> ion release then slowed, and after ca. 24 h appeared to reach an equilibrium concentration value (Figure 5). At this time point, ca. 35% and 38% of the original Ag<sup>+</sup> content of BSA/GLA/Ag<sup>+</sup>(0.01) and BSA/GLA/Ag<sup>+</sup>(0.001), respectively, had been released into the supporting electrolyte solution. The extent of Ag<sup>+</sup> ion leaching from the BSA/GLA hydrogels was not too dissimilar to that reported by Babu et al. [37] for their polyethyleneglycol- or lactose-backbone-based 3,4-dihydroxyphenyl-L-alanine polymer gels (57 and 44%, respectively, after 24 h).

The antimicrobial activity of the alginate and BSA/GLA samples was assessed using a plate method and by measuring the zone of microbial growth inhibition following incubation at 37 °C for 24 h (Table 3). No growth inhibitory effects were observed when the organisms were challenged with CaALG, CaALG/PGA/HSA, and BSA/GLA hydrogels, which had no added Ag<sup>+</sup> ions. In contrast, as previously observed by Kim et al., CaALG/QA beads, which contain quaternary ammonium groups but are devoid of Ag<sup>+</sup> ions, displayed broad spectrum antimicrobial activity but were more active against gram positive rather than gram negative bacteria [32]. Disinfectants containing quaternary ammonium salts are known to be quite toxic toward a host of bacterial species [38,39], an action thought to be mediated through the binding of the cationic ammonium moiety to anionic locations on the outer surface of bacteria.

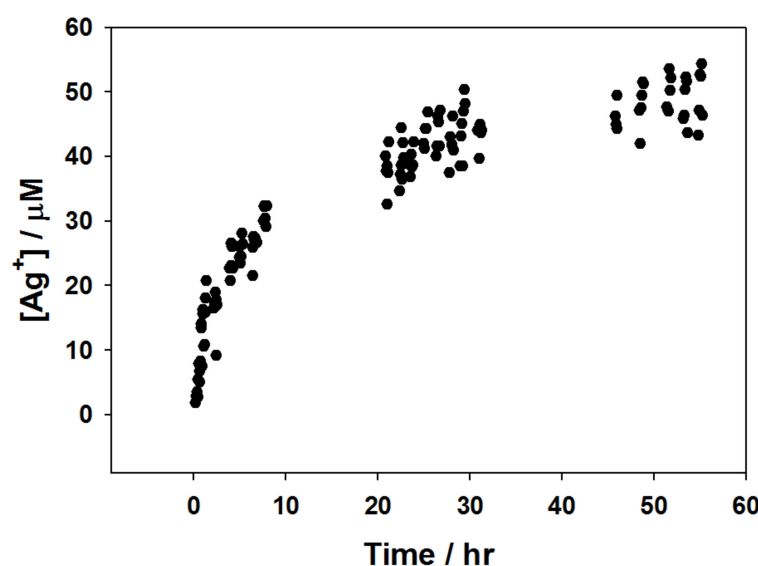


**Figure 5.** Concentration of  $\text{Ag}^+$  ions released into aqueous 0.2 M  $\text{NaNO}_3$  supporting electrolyte obtained using electrochemical determination from a BSA/GLA/ $\text{Ag}^+$ (0.01) hydrogel disk over a 55 h period. The stripping peak currents were normalised with respect to deposition times and  $\text{Ag}^+$  concentrations determined using the averaged normalised calibration curve parameters.

**Table 3.** Antimicrobial growth inhibition zones ( $\text{mm}^2$ ) \*.

Polymeric Material	<i>C. albicans</i>	MRSA	<i>S. aureus</i>	<i>E. coli</i>	<i>P. aeruginosa</i> 10145	<i>P. aeruginosa</i> 27853
CaALG (no $\text{Ag}^+$ )	0 *	0	0	0	0	0
CaALG/ $\text{Ag}^+$ (0.01)	d.i. *	23	19	31	17	23
CaALG/ $\text{Ag}^+$ (0.1)	83	99	21	39	21	30
CaALG/PGA/HSA (no $\text{Ag}^+$ )	0	0	0	0	0	0
CaALG/PGA/HSA/ $\text{Ag}^+$ (0.01)	d.i.	16	19	21	24	16
CaALG/PGA/HSA/ $\text{Ag}^+$ (0.1)	143	31	28	23	26	19
CaALG/QA (no $\text{Ag}^+$ )	24	d.i	18	d.i	35	d.i
CaALG/QA/ $\text{Ag}^+$ (0.01)	14	13	59	23	56	d.i
CaALG/QA/ $\text{Ag}^+$ (0.1)	306	46	76	84	106	20
BSA/GLA (no $\text{Ag}^+$ )	0	0	0	0	0	0
BSA/GLA/ $\text{Ag}^+$ (0.001)	d.i.	23	26	35	38	38
BSA/GLA/ $\text{Ag}^+$ (0.01)	d.i.	31	36	41	49	58

\* d.i.—direct inhibition. No microbial growth was observed in the region of the plate below the beads or on the beads but there was no zone of inhibition surrounding the beads. Zero inhibition zone—microbial growth was observed under and on top of the beads.

All of the  $\text{Ag}^+$ -containing gel samples registered some degree of microbial growth inhibition. For the three sets of alginate pairings, it was generally found that the samples prepared using the higher concentrations of  $\text{AgNO}_3$  showed superior activity against most (but not all) of the microbes. This trend is likely due to the greater amounts of  $\text{Ag}^+$  ions having diffused into the surrounding media as predicted on the basis of the leaching studies, and mirrors that reported by Lansdown [17], and also by Castellano et al. [40], who studied the antibacterial activity of eight, commercially available,  $\text{Ag}^+$ -containing wound dressings. In the current study, there was a less significant improvement in activity on going from BSA/GLA/ $\text{Ag}^+$ (0.001) to BSA/GLA/ $\text{Ag}^+$ (0.01).

The three alginate samples which were prepared using 0.1 M  $\text{AgNO}_3$  were particularly destructive to the *C. albicans* fungal cells, with CaALG/QA/ $\text{Ag}^+$ (0.1) producing the largest effect: an inhibition zone of 306  $\text{mm}^2$ . In contrast, the two BSA/GLA/ $\text{Ag}^+$  samples only inhibited growth at the points of direct contact with the fungus, implying that in these cases, there was no diffusion of  $\text{Ag}^+$ .

In general, the Ag<sup>+</sup> hydrogels displayed moderate to good antibacterial activity, without any clear bias between gram-positive and gram-negative organisms, despite the very different cell wall compositions of these classes of bacteria. Ag<sup>+</sup>-free and Ag<sup>+</sup>-containing CaALG/QA samples exerted a significant degree of selectivity between the two strains of *P. aeruginosa*, being strikingly more active against the 10,145 strain. On the other hand, BSA/GLA/Ag<sup>+</sup>(0.01) was markedly better than any of the other test materials against *P. aeruginosa* 27,853. CaALG/Ag<sup>+</sup>(0.1) was unrivalled in its highly detrimental effect on gram-positive MRSA. A serious concern with using alginate hydrogels in wound dressings is the low stability of the hydrogel upon swelling, which occurs upon loss of the 3-D network. This can lead to a burst release of a bioactive species trapped within the hydrogel [41,42]. In this regard, the modified alginate beads have the more attractive features; they exhibited decreased water absorption properties compared to the CaALG beads in 1% w/v NaCl solution. In addition, when the beads were placed in the nutrient solution used to grow the microbes and shaken at 30 °C for 24 h, it was observed that after 6 h the silver ion impregnated CaALG beads had disintegrated, while the analogous CaALG/QA CaALG/PGA/HSA beads, even though hugely swollen, were still intact at the 24 h time mark.

#### 4. Conclusions

We have shown that Ag<sup>+</sup>-containing, functionalised alginates and BSA/GLA hydrogels are readily prepared using cheap, readily available starting materials, and offer good growth inhibition across a broad range of microbial pathogens. Alginate containing a pendant quaternary ammonium (QA) group is bioactive in the absence of added Ag<sup>+</sup> ion; interestingly, incorporation of Ag<sup>+</sup> significantly augments this activity. Both the CaALG/PGA/HSA and CaALG/QA show reduced swelling in water and saline solution compared to the CaALG beads, and therefore have greater potential for application as a wound dressing incorporating bioactive agents. Regarding their potential use in the clinic, as either a dermal wound antiseptic matrix or an antiseptic-enriched tissue adhesive, both the alginate and BSA/GLA Ag<sup>+</sup>-containing gels exert an oligodynamic effect (bioactive at very low concentration) through the slow and continuous release of antimicrobial Ag<sup>+</sup> ions, and effectively reduce bioburden. The hydrogel systems based on biological macromolecules described here have the potential to minimise the risk of silver toxicity while maintaining antimicrobial properties, as the silver can be released in small amounts. Additionally, the hydrogel materials retain a reservoir of Ag<sup>+</sup> ions which should be sufficient to afford the ongoing sterility of the materials themselves.

**Supplementary Materials:** Available online at <https://www.mdpi.com/article/10.3390/chemistry3020047/s1> are Figures S1–S6. Contains a calibration curve and examples of typical data associated with the electrochemical determination of the leaching of Ag<sup>+</sup> from the BSA/GLA/Ag<sup>+</sup>(0.001) and BSA/GLA/Ag<sup>+</sup>(0.01) and FTIR of the CaALG/QA compared to the starting materials and EDX spectra to show the impregnation of Ag<sup>+</sup> into the alginate beads.

**Author Contributions:** Investigation, L.G. and A.S.; supervision and funding acquisition, K.K.; conceptualization, M.D.; investigation and writing—original draft preparation, J.C.; supervision and funding acquisition, C.B.; conceptualization and funding acquisition, K.G.R.; supervision and writing—original draft preparation, M.M.; supervision, funding acquisition and writing—original draft preparation, A.D.R. All authors have read and agreed to the published version of the manuscript.

**Funding:** This research was funded by PRTL strand IV, Monaghan County Council and the Irish Department of Agriculture, Food and the Marine (DAFM) (Research Stimulus Fund Programme—RSF 07545).

**Institutional Review Board Statement:** Not applicable.

**Informed Consent Statement:** Not applicable.

**Data Availability Statement:** Not applicable.

**Conflicts of Interest:** The authors declare no conflict of interest.

## References

1. Kirschning, A.; Dibbert, N.; Draeger, G. Chemical functionalization of polysaccharides-towards biocompatible hydrogels for biomedical applications. *Chem. Eur. J.* **2018**, *24*, 1231–1240. [CrossRef]
2. Kothale, D.; Verma, U.; Dewangan, N.; Jana, P.; Jain, A.; Jain, D. Alginate as Promising Natural Polymer for Pharmaceutical, Food, and Biomedical Applications. *Curr. Drug Deliv.* **2020**, *17*, 755–775. [CrossRef]
3. Lantigua, D.; Nguyen, M.A.; Wu, X.; Suvarnapathaki, S.; Kwon, S.; Gavin, W.; Camci-Unal, G. Synthesis and characterization of photocrosslinkable albumin-based hydrogels for biomedical applications. *Soft Matter* **2020**, *16*, 9242–9252. [CrossRef]
4. Nogueira, G.F.; Augustus de Oliveira, R.; Velasco, J.I.; Fakhouri, F.M. Methods of incorporating plant-derived bioactive compounds into films made with agro-based polymers for application as food packaging: A brief review. *Polymers* **2020**, *12*, 2518. [CrossRef]
5. Ahmed, S.; Ikram, S. In situ nanosilver-immobilized chitosan/oxidized carboxymethylcellulose blend dressings for wound management. *Biopolym. Biomat.* **2019**, 231–252.
6. Sabourian, P.; Tavakolian, M.; Yazdani, H.; Frounchi, M.; van de Ven, T.G.M.; Maysinger, D.; Kakkar, A. Stimuli-responsive chitosan as an advantageous platform for efficient delivery of bioactive agents. *J. Control Release* **2020**, *317*, 216–231. [CrossRef]
7. Viganor, L.; Howe, O.; McCarron, P.; McCann, M.; Devereux, M. The Antibacterial Activity of Metal Complexes Containing 1,10-Phenanthroline: Potential as Alternative Therapeutics in the Era of Antibiotic Resistance. *Curr. Top. Med. Chem.* **2017**, *17*, 1280–1302. [CrossRef]
8. Porter, G.C.; Schwass, D.R.; Tompkins, G.R.; Bobbala, S.K.R.; Medlicott, N.J.; Meledandri, C.J. AgNP/Alginate Nanocomposite hydrogel for antimicrobial and antibiofilm applications. *Carbohydr. Polym.* **2021**, *251*, 117017. [CrossRef]
9. Cao, Z.; Luo, Y.; Li, Z.; Tan, L.; Liu, X.; Li, C.; Zheng, Y.; Cui, Z.; Yeung, K.W.K.; Liang, Y.; et al. Antibacterial Hybrid Hydrogels. *Macromol. Biosci.* **2021**, *21*, 2000252. [CrossRef]
10. Chalitangkoon, J.; Wongkittisin, M.; Monvisade, P. Silver loaded hydroxyethylacryl chitosan/sodium alginate hydrogel films for controlled drug release wound dressings. *Int. J. Biol. Macromol.* **2020**, *159*, 194–203. [CrossRef]
11. McCann, M.; Geraghty, M.; Devereux, M.; O'Shea, D.; Mason, J.; O'Sullivan, L. Insights into the Mode of Action of the Anti-*Candida* Activity of 1,10-Phenanthroline and its Metal Chelates. *Metal Based Drugs* **2000**, *7*, 185–193. [CrossRef] [PubMed]
12. Coyle, B.; Kavanagh, K.; McCann, M.; Devereux, M.; Geraghty, M. Mode of Anti-Fungal Activity of 1,10-Phenanthroline and its Cu(II), Mn(II) and Ag(I) Complexes. *BioMetals* **2003**, *16*, 321–329. [CrossRef]
13. Kelly, J.; Rowan, R.; McCann, M.; Kavanagh, K. Exposure to Caspofungin activates Cap and Hog pathways in *Candida albicans*. *Med. Mycol.* **2009**, *47*, 697–706. [CrossRef] [PubMed]
14. Rowan, R.; McCann, M.; Kavanagh, K. Analysis of the Response of *Candida albicans* to Silver(I). *Med. Mycol.* **2010**, *48*, 498–505. [CrossRef]
15. Smith, A.; McCann, M.; Kavanagh, K. Proteomic analysis of the proteins released from *Staphylococcus aureus* following exposure to Ag(I). *Toxicol. In Vitro* **2013**, *27*, 1644–1648. [CrossRef]
16. Smith, A.; Rowan, R.; McCann, M.; Kavanagh, K. Exposure of *Staphylococcus aureus* to silver(I) induces a short term protective response. *BioMetals* **2012**, *25*, 611–616. [CrossRef]
17. Lansdown, A.B.G.; Williams, A. How safe is silver in wound care? *J. Wound Care* **2004**, *13*, 131–136. [CrossRef]
18. Venugopal, B.; Luckey, T.D. *Metal Toxicity in Mammals-2: Chemical Toxicity of Metals and Metalloids*; Plenum Press: New York, NY, USA, 1978; p. 35.
19. Migneault, I.; Dartiguenave, C.; Bertrand, M.J.; Waldron, K.C. Glutaraldehyde: Behavior in aqueous solution, reaction with proteins, and application to enzyme crosslinking. *Biotechniques* **2004**, *37*, 790–802. [CrossRef]
20. Wine, Y.; Cohen-Hadar, N.; Freeman, A.; Frolow, F. Elucidation of the mechanism and end products of glutaraldehyde crosslinking reaction by X-ray structure analysis. *Biotechnol. Bioeng.* **2007**, *98*, 711–718. [CrossRef]
21. Cryolife. Available online: <http://www.cryolife.com/products/bioglue-surgical-adhesive> (accessed on 7 February 2021).
22. Mitrev, Z.; Belostotskii, V.; Hristov, N. Suture line reinforcement using suction-assisted bioglue application during surgery for acute aortic dissection. *Interact Cardiovasc Thorac Surg.* **2007**, *6*, 147–149. [CrossRef]
23. Bhamidipati, C.M.; Coselli, J.S.; LeMaire, S.A. BioGlue® in 2011: What Is Its Role in Cardiac Surgery? *J. Extra Corpor Technol.* **2012**, *44*, 6–12.
24. Gaberel, T.; Borgey, F.; Thibon, P.; Lesteven, C.; Lecoutour, X.; Emery, E. Surgical site infection associated with the use of bovine serum albumine-glutaraldehyde surgical adhesive (BioGlueA (R)) in cranial surgery: A case-control study. *Acta Neurochir.* **2011**, *153*, 156–162. [CrossRef] [PubMed]
25. Appropriate Use of Silver Dressings in Wounds. Available online: <https://www.woundsinternational.com/resources/details/international-consensus-appropriate-use-silver-dressings-wounds-english-en> (accessed on 1 March 2021).
26. Holt, K.B.; Bard, A.J. Interaction of Silver(I) Ions with the Respiratory Chain of *Escherichia coli*: An Electrochemical and Scanning Electrochemical Microscopy Study of the Antimicrobial Mechanism of Micromolar Ag<sup>+</sup>. *Biochemistry* **2005**, *44*, 13214–13223. [CrossRef]
27. Rousseau, I.; Le Cerf, D.; Picton, L.; Argillier, J.F.; Muller, G. Entrapment and release of sodium polystyrene sulfonate (SPS) from calcium alginate gel beads. *Eur. Polym. J.* **2004**, *40*, 2709–2715. [CrossRef]
28. McEntee, M.K.E.; Bhatia, S.K.; Tao, L.; Roberts, S.C.; Bhatia, S.R. Tunable transport of glucose through ionically-crosslinked alginate gels: Effect of alginate and calcium concentration. *J. Appl. Polym. Sci.* **2008**, *107*, 2956–2962. [CrossRef]

29. Isiklan, N. Controlled release study of carbaryl insecticide from calcium alginate and nickel alginate hydrogel beads. *J. Appl. Polym. Sci.* **2007**, *105*, 718–725. [[CrossRef](#)]
30. Sarker, D.K.; Wilde, P.J. Restoration of protein foam stability through electrostatic propylene glycol alginate-mediated protein-protein interactions. *Colloids Surf. B* **1999**, *15*, 203–213. [[CrossRef](#)]
31. Edwards-Levy, F.; Levy, M.C. Serum albumin-alginate coated beads: Mechanical properties and stability. *Biomaterials* **1999**, *20*, 2069–2084. [[CrossRef](#)]
32. Kim, Y.S.; Kim, H.W.; Lee, S.H.; Shin, K.S.; Hur, H.W.; Rhee, Y.H. Preparation of alginate-quaternary ammonium complex beads and evaluation of their antimicrobial activity. *Int. J. Biol. Macromol.* **2007**, *41*, 36–41. [[CrossRef](#)]
33. Chen, S.-C.; Wu, Y.-C.; Mi, F.-L.; Lin, Y.-H.; Yu, L.-C.; Sung, H.-W. A novel pH-sensitive hydrogel composed of N,O-carboxymethyl chitosan and alginate cross-linked by genipin for protein drug delivery. *J. Control. Release* **2004**, *96*, 285–300. [[CrossRef](#)]
34. Abd El-Ghaffar, M.A.; Hashem, M.S.; El-Awady, M.K.; Rabie, A.M. pH-sensitive sodium alginate hydrogels for riboflavin controlled release. *Carbohydr. Polym.* **2012**, *89*, 667–675. [[CrossRef](#)] [[PubMed](#)]
35. Deen, G.R. Swelling Behavior of Metal-Ion Uptake Capacity of pH-Responsive Hydrogels of Poly(N-acryloyl-N'-ethylpiperazine). *J. Dispersion Sci. Technol.* **2010**, *31*, 1673–1678. [[CrossRef](#)]
36. Ma, X.; Sun, X.; Hargrove, D.; Chen, J.; Song, D.; Dong, Q.; Lu, X.; Fan, T.-H.; Fu, Y.; Lei, Y. A Biocompatible and Biodegradable Protein Hydrogel with Green and Red Autofluorescence: Preparation, Characterization and In Vivo Biodegradation Tracking and Modeling. *Sci. Rep.* **2016**, *6*, 19370. [[CrossRef](#)] [[PubMed](#)]
37. Babu, R.; Zhang, J.; Beckman, E.J.; Virji, M.; Pasculle, W.A.; Wells, A. Antimicrobial activities of silver used as a polymerization catalyst for a wound-healing matrix. *Biomaterials* **2006**, *27*, 4304–4314. [[CrossRef](#)] [[PubMed](#)]
38. Fazlara, A.; Ekhtelat, M. The disinfectant effects of Benzalkonium chloride on some important foodborne pathogens. *Am. Eurasian J. Agric. Environ. Sci.* **2012**, *12*, 23–29.
39. Tawfik, S.M.; Abd-Elaal, A.A.; Shaban, S.M.; Roshdy, A.A. Surface, thermodynamic and biological activities of some synthesized Gemini quaternary ammonium salts based on polyethylene glycol. *J. Ind. Eng. Chem.* **2015**, *30*, 112–119. [[CrossRef](#)]
40. Castellano, J.J.; Shafii, S.M.; Ko, F.; Donate, G.; Wright, T.E.; Mannari, R.J.; Payne, W.G.; Smith, D.J.; Robson, M.C. Comparative evaluation of silver-containing antimicrobial dressings and drugs. *Int. Wound J.* **2007**, *4*, 114–122. [[CrossRef](#)]
41. Straccia, M.C.; Gomez d' Ayala, G.; Romano, I.; Oliva, A.; Laurienzo, P. Alginate Hydrogels Coated with Chitosan for Wound Dressing. *Mar. Drugs* **2015**, *13*, 2890–2908. [[CrossRef](#)]
42. Aderibigbe, B.A.; Buyana, B. Alginate in Wound Dressings. *Pharmaceutics* **2018**, *10*, 42. [[CrossRef](#)]